A NEW SCHEME FOR AUTOMATIC INITIALIZATION OF DEFORMABLE MODELS

Weijia Shen and Ashraf A. Kassim

National University of Singapore
Department of Electrical & Computer Engineering
10 Kent Ridge Crescent, Singapore 119260
{shenweijia, ashraf}@nus.edu.sg

ABSTRACT

This paper presents a novel scheme for automatic initialization for all types of deformable models. Our method is able to automatically generate a close-to-boundary initialization which is independent of the subsequent segmentation process. Therefore, our method enables different types of deformable models achieve more accurate and robust results. Topographic Independent Component Analysis (TICA) based feature exaction technique is presented for learning a representation from a set of un-labeled image patches. During learning, a topographic map of basis components emerge. An intelligent contour generation procedure is also proposed. Experimental results on abdominal CT images demonstrate the potential of our approach.

Index Terms— Automatic initialization, Deformable models, Topographic ICA, CT images

1. INTRODUCTION

Segmentation of anatomical structures from medical images is often the first step in computer aided diagnosis. Further analysis highly depends on the quality of the segmented structures. In recent years, geometric deformable models, or level set methods [1][2], have been applied to medical image segmentation with considerable success. Compared with the parametric deformable model, which is also known as snakes or active contours [3], geometric deformable models are superior in many aspects and especially in handling topological changes.

However, for both parametric or geometric deformable models, an contour initialization is still required. This initialization is a major drawback of parametric models since its capture range is very limited [14]. Although Xu [13] introduces the gradient vector flow (GVF) which increases the capture range of a classic snake, the result could become unacceptable under a slightly different initialization [6]. Even with geometric deformable models, contour initializations still biases the final results [14]. Furthermore, a segmentation process with an contour initialization that is not close to the boundary/surface will take a very long time to converge to the right state, especially in 3D cases [14].

A number of methods have been proposed ([4], [5], [6], [7]) to solve the initialization problem. Tauber et al. [6] attempted to utilize gradient vector flow to pre-segment the image to obtain an initialization, while others tried to locate the initial contour by subtracting two adjacent images from sequence images [7]. Some tried to use edge-detection or revise the snake energy function [5]. Most initialization approaches are highly dependant on specific segmentation techniques or specific properties of the data sets. In the meantime, few of these methods have used prior knowledge to guide the initialization process [14].

In this paper, we introduce a novel scheme to obtain an automatic initialization using prior knowledge. Unlike existing techniques, our method is independent of the subsequent segmentation process and thus could be used for all segmentation methods based on deformable models. Prior knowledge is incorporated naturally by a classification procedure.

The rest of the paper is organized as follows. In Section 2, we describe the proposed scheme for automatic contour initialization with the usage of prior knowledge. In Section 3, experimental results on abdominal CT images are presented and discussed.We provide our conclusions in Section 4.

2. AN OVERVIEW OF THE PROPOSED METHOD

As detailed in the following sub-sections, our proposed scheme involves three stages: 1. feature exaction and training, 2. patch classification and 3. intelligent patch linking and contour generation.

2.1. ICA-based modeling and subspace learning

Numerous techniques have been developed to extract features from a set of training data. Principle component analysis (PCA) is a popular unsupervised statistical method which is able to learn useful data representations. It is often used to find a basis set which is determined by the dataset itself. However, it can only decorrelate second order moments ([15], [16]) and important high-order relationships in a image will be ignored. The more recent independent component analysis (ICA)

is able to impose higher-order independence [17]. In [16], it is shown that the trained ICA face representations were superior to representations based on PCA for face recognitions.

In classic ICA, the basic model is constructed as a gray-level image $I(x, y)$ which is a linear superposition of basis functions $b_i(x, y)$,

$$I(x, y) = \sum_{i=1}^{m} b_i(x, y)s_i, \tag{1}$$

where $\mathbf{s} = (s_1, s_2, \ldots, s_m)$ are stochastic coefficients, that are different for each $I(x, y)$. Given a sufficient number of image patches $I(x, y)$ in practice, the values of s_i and $b_i(x, y)$ for all i and (x, y) need to be determined/estimated. If we restrict $b_i(x, y)$ to form an invertible linear system, then this system can be inverted as

$$s_i = \langle \omega_i, I \rangle \tag{2}$$

where the ω_i denote the inverse filters and $\langle \omega_i, I \rangle$ denotes the dot-product. The underlying assumption is that s_i are mutually independent random variables.

Topographic ICA(TICA) [11] is an extension to the classic ICA.In classic ICA, due to the independence assumption, the independent components s_i have no particular order or other relationships. However, in real applications, some estimated independent components are dependent [15]. In TICA, this assumption is relaxed. Components within a small neighborhood are allowed to be correlated in their energies. A neighborhood system [11] is adopted to define the range of dependency. The topographic ordering is defined by the correlations between the energies of the components [11].

$$cov(s_i^2, s_j^2) = E\{s_i^2 s_j^2\} - E\{s_i^2\}E\{s_j^2\} \tag{3}$$

Estimating a TICA model can be achieved by maximizing a likelihood function [11].As for implementation, we choose one among the various algorithms available. The TICA software downloaded from http://www.cs.helsinki.fi/u/phoyer/ is used.

In our scheme, the training data set consists of a series of gray-scale training images (N by N), each with its manual segmentation result stored in a separate black & white image.

Instead of resizing the training image to a $M\times$ M pixel image, the input data $I_k(x, y)$ are obtained by taking all $M \times M$ pixel image patch from all training images. Thereafter, each image patch is converted to a vector using the row major representation.

Before the exaction of independent components, the input data $I_k(x, y)$needs to be preprocessed. It involves whitening and dimension reduction using PCA. First, the mean gray-scale value of each image patch was subtracted first. Then, the data are low-pass filtered by reducing the dimension of the vector by PCA. Next, the correlations between the components of the data are removed by multiplying the data by $\mathbf{C}^{-1/2}$, where $\mathbf{C}$ is the covariance of the data obtained from PCA.

2.2. Patch classification

After the unsupervised extraction of independent components using TICA, the estimated independent components will serve as filters to extract features from image patches. Although many sophisticated methods could be applied for patch classification,the results shown in this paper adopt the simplest possible classifier:nearest neighbor classifier. This is to show that the filters learned are optimal and this scheme is not fully dependent on the patch classification stage.With more advanced classifiers, the classification performance are bound to improve.

After a test image is presented, and the goal is to segment the object of interest. First, all the $M \times M$ image patches are sequentially taken out. Each patch will be converted to a row vector. Let it be referred to as $\mathbf{x}$. Suppose $\mathbf{s} = [\mathbf{s}_1\ \mathbf{s}_2\ \ldots\ \mathbf{s}_m]^T$ is the matrix containing the independent components and $\omega = [\omega_1\ \omega_2\ \ldots\ \omega_m]$ is the weight vector. Then

$$\mathbf{x} = \omega_1\mathbf{s}_1 + \omega_2\mathbf{s}_2 + \ldots + \omega_m\mathbf{s}_m. \tag{4}$$

By solving this equation, ω could be determined.

Using the manual segmentation results for each training image, we could label every training image patch. Suppose we name those patches containing a portion of object boundary contour-patches, those without any part of the boundary background-patches. Then we could classify any new image patch x into contour-patch class or background-patch class using nearest neighbor classifier by comparing the Euclidean distances between $\omega_{\mathbf{x}}$ and ω_i from labeled image patches.

2.3. Intelligent patch linking and contour generation

With sufficient training examples, most background patches and most contour patches will be correctly recognized. If we let the labeled contour patch to be painted white. As can be observed from Fig.2(b), most misclassified background patches are not adjacent to each other(*i.e.*,they are not neighbors under the 4-neighbor definition or the 8-neighbor definition). Even when they are adjacent, they can only form a small connected group under a 4-neighbor or an 8-neighbor definition. This phenomenon could be theoretically expected since it is less probable the false-negative patches or the false-positive patches can form large connected groups and make a meaningful representation accordingly.

Inspired by this observation, the first step of processing is to identify all connected groups for all the white patches (contour patches) under a user-specified neighbor definition. In this paper, we choose 8-neighbor definition since it could describe all the possible relationships between neighboring contour patches. Different connected groups could be regarded as different islands. Large island has a high probability to be a

the true contour patch islands while smaller islands or even one-patch islands are more likely to be a false-positive error. According to this, we will set a threshold on the size of the islands. If the size of one island is above this threshold, it will survive.

After this procedure, only big islands survive. As in binary image processing,a thinning operation is then applied on each island (patches are treated as pixels) to remove the ambiguity for the contour generation processes. To generate a close initial contour, they are connected together by linking the closest endings of each thinned islands (Fig. 2). For simplicity, we link the centers of two patches using a straight line. Next, another thinning operation is performed to make sure there is no ambiguity.

The problem now has been transformed to how to generate an initial contour from a group of connected patches. Numerous methods could be developed to create a curve.In our experiment, we simply link the geometric centers of every two adjacent rectangular patches. For a more sophisticated and smoother contour, we could use spline fitting techniques [18].In the next section, we are showing an example of applying our scheme for spleen segmentation on abdominal CT images.

3. APPLICATION TO ABDOMINAL CT IMAGES

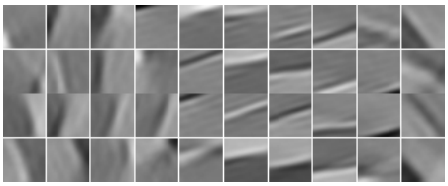

Fig. 1. Example of placing a figure with experimental results.

A set of 30 abdominal CT images (512×512) with manual segmentation results were used. 10 images were randomly selected from 30 images and are treated as training images. The rest 20 images served as test images. The size of each image patch was experimentally set to 32×32 pixels. All image patches were taken out from the training sets and each patch was then arranged into one row. Mean gray-value of each patch are subtracted. Then,the dimension of each vector was then reduced to 160 by PCA. TICA was then performed on a set of $16 \times 16 \times 10 = 2560$ patches.

Fig. 1 shows 40 learned independent components (basis).As can be seen, meaningful independent components emerge from unsupervised training on all image patches. Every four basis from the same column span a small subspace. They look much similar to each other than to basis from other columns. All the 40 basis are used to exact features from a test image patch. Table 1 gives the classification rate on all the test image patches using a simple nearest neighboring classifier. The classification rate is slightly higher for background patches. It may contribute to that there are much more training examples available for background patches than for contour patches.

Table 1. IMAGE PATCH CLASSIFICATION RATE

Contour Patches	Background Patches
90.8%	93.6%

Fig. 2 shows different stages of generating an automatic initialization contour on a test image. As can be observed,noise and ambiguity are successfully removed by our smart patch linking method. The simple polygon contour shown in Fig. 2(e) is very close to the boundary and therefore resembles the final segmentation result shown in Fig. 2(f). The final result shown in Fig. 2(f) is obtained using GVF snake [13]. Other methods, like Level set based methods could be used as well.

4. DISCUSSIONS AND CONCLUSION

In this paper, we introduce a method which is able to automatically generate an initial contour with prior knowledge and which is naturally incorporated through a TICA-based learning and feature exaction scheme through the labeling/recognition process.With TICA-based basis learning and feature exaction, the high-order relationships are easily explored and the learned independent components are "customized" to the training data sets used. Our scheme is mainly designed for situations where a close to boundary initialization contour is required. With our scheme, algorithms that are sensitive to initializations are able to achieve more accurate and robust results. Good results are obtained when our method is applied on spleen segmentation on CT images. Since this approach is independent of the subsequent process, it can be applied to any segmentation methods that requires initialization.

5. REFERENCES

[1] S. Osher and J. A. Sethian, Fronts propagating with curvaturedependent speed: Algorithms based on Hamilton-Jacobi formulations, *J. Comp. Phy.*, vol. 79, pp. 12C49, 1988.

[2] R.Malladi, J. A. Sethian, and B. C. Vermuri, Shape modeling with front propagation: A level set approach, *IEEE Trans. Pattern Anal. and Machine Intell.*, vol. 17, no. 2, pp. 158C174, 1995.

[3] M. Kass, A. Witkin, and D. Terzopoulos, Snakes: Active contour models, *Int. J. Computer Vision*, vol. 1, no. 4, pp. 321C331, 1987.

[4] Carrara M, Tomatis S, Bono A, Bartoli C, Moglia D, Lualdi M, Colombo A, Santinami M, and Marchesini R, "Automated segmentation of pigmented skin lesions in multispectral imaging," *Phys Med Biol.*,2005

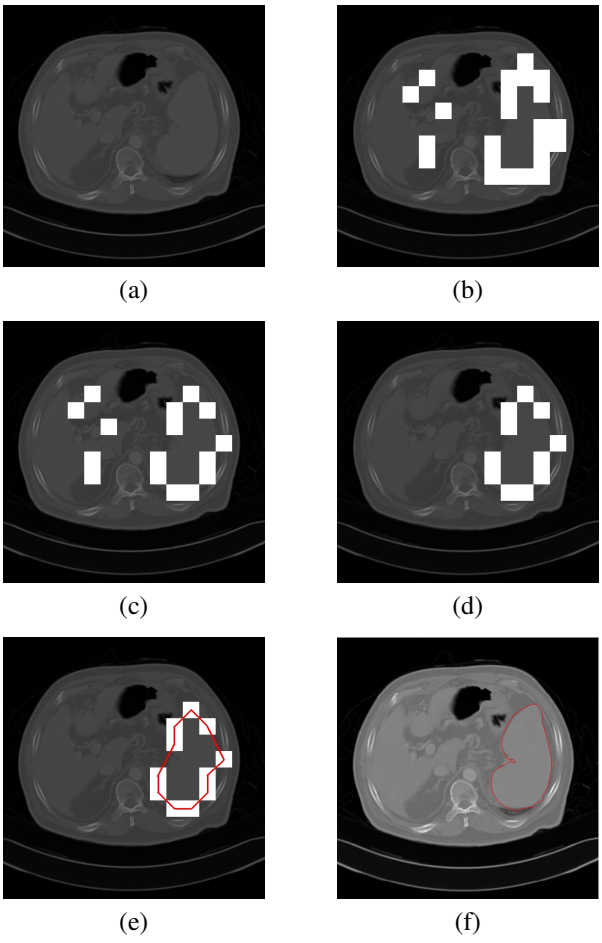

Fig. 2. Different stages of generating an automatic initialization contour on a test image. (a) Original test image. (b)Patch classification result, contour patches are in white. (c) Thinning results of contour patches in (b). (d) Removing small islands by thresholding. (e) Patch linking and initial contour generation (shown in red). (f) Final result shown in red using GVF snake.

[5] Medina, V.B. , Valdes, R.C. , Yanez-Suarez, O. , Garza-Jinich, M. and Lerallut, J.-F. ,"Automatic initialization for a snakes-based cardiac contour extraction," *Proceedings of the 22nd Annual International Conference on Engineering in Medicine and Biology Societyvol*, vol. 3, pp.1625-1628,2000

[6] Clovis Tauber, Batatia, H. and Ayache, A. , "A general quasi-automatic initialization for snakes: application to ultrasound images," *IEEE International Conference on Image Processing*,vol. 2 pp. 806-9 2005.

[7] Pluempitiwiriyawej, C. and Sotthivirat, S.,"Active Contours With Automatic Initialization For Myocardial Perfusion Analysis," *27th Annual International Conference of the on Engineering in Medicine and Biology Society*, pp.3332- 3335, 2005.

[8] V. Caselles, R. Kimmel, and G. Sapiro, Geodesic active contours, Int. *J. Computer Vision*, vol. 22, no. 1, pp. 61C79, 1997.

[9] T. F. Cootes, C. J. Taylor, D. H. Cooper, and J. Graham, Active shape models C their training and application, *Comput. Vision Image Understand.*, vol. 61, no. 1, pp. 38C59, Jan. 1995.

[10] M. E. Leventon, W. E. L. Grimson, and O. Faugeras, Statistical shape influence in geodesic active contours, in *Proc. IEEE Conf. Computer Vision and Pattern Recognition*, vol. 1, pp. 316C323,2000.

[11] A. Hyvärinen, P. O. Hoyer and M. Inki, "Topographic Independent Component Analysis," *Neural Computation*, vol. 13(7), pp.1527-1558, 2001.

[12] A. Hyvärinen and P. O. Hoyer, "Emergence of Phase and Shift Invariant Features by Decomposition of Natural Images into Independent Feature Subspaces," *Neural Computation*, vol. 12(7), pp.1705-1720, 2000.

[13] C.Xu and J.L. Prince, "Snakes, shapes and gradient vector flow", *IEEE Trans. on Image Proc.*, vol. 7, pp.359-369,1998.

[14] J. Suri, K. Liu, S. Singh, S. Laxminarayana, and L. Reden, Shape recovery algorithms using level sets in 2-D/3-D medical imagery: A state-of-the-art review, *IEEE Trans. Inform. Technol. Biomed.*, vol. 6, pp. 8C28, 2002.

[15] Stan Z Li , XiaoGuang Lu , Xinwen Hou , Xianhua Peng and Qiansheng Cheng,"Learning multiview face subspaces and facial pose estimation using independent component analysis," *IEEE Trans. on Image Proc.*, vol. 14, pp.705-712, 2005.

[16] Bartlett, M.S. , Movellan, J.R. and Sejnowski, T.J. , "Face recognition by independent component analysis," *IEEE Trans. on Neural Networks*, vol. 13, pp. 1450- 1464, 2002.

[17] P. Comon, "Independent component analysis-A new concept?"," *Signal Processing*,vol. 36, pp.287-314,1994.

[18] Farzin Mokhtarian, Yoke Khim Ung and Zhitao Wang, "Automatic fitting of digitised contours at multiple scales through the curvature scale space technique," *Computers & Graphics*,vol. 29, pp.961-971, 2005